RAA 2019 Vol. **19** No. **2**, 29(10pp) doi: 10.1088/1674–4527/19/2/29

http://www.raa-journal.org *http://iopscience.iop.org/raa*

Research in Astronomy and Astrophysics

A compilation of known QSOs for the *Gaia* mission

Shi-Long Liao[1,2], Zhao-Xiang Qi[1,2], Su-Fen Guo[1,2] and Zi-Huang Cao[3]

[1] Shanghai Astronomical Observatory, Chinese Academy of Sciences, Shanghai 200030, China; *shilongliao@shao.ac.cn*

[2] School of Astronomy and Space Science, University of Chinese Academy of Sciences, Beijing 100049, China

[3] National Astronomical Observatories, Chinese Academy of Sciences, Beijing 100101, China

Received 2018 April 17; accepted 2018 September 5

Abstract Quasars are essential for astrometry in the sense that they are spatially stationary because of their large distance from the Sun. The European Space Agency (ESA) astrometric satellite *Gaia* is scanning the whole sky with unprecedented accuracy up to the level of a few μas. However, *Gaia*'s two-fields-of-view-observation strategy may introduce a parallax bias in the *Gaia* catalog. Since it presents no significant parallax, a quasar is the perfect natural object to detect such bias. More importantly, quasars can be used to construct a celestial reference frame in the optical wavelengths for the *Gaia* mission. In this paper, we compile a list of known quasars that have been published in the literatures. The final compilation (designated as Known Quasars Catalog for *Gaia* mission, KQCG) contains 1 842 076 objects, among which 797 632 objects are found in *Gaia* DR1 after cross-identifications. Redshift, color information and position uncertainties of the objects are also provided if available. This catalog will be very useful for the *Gaia* mission.

Key words: quasars: general — astrometry — parallaxes — proper motions — reference systems — catalogs

1 INTRODUCTION

The European Space Agency's (ESA's) *Gaia* mission, launched in 2013, is a space-based astrometric, photometric and radial velocity all-sky survey at optical wavelengths (Gaia Collaboration et al. 2016b). As the successor to the *Hipparcos* mission (Perryman et al. 1997), *Gaia* will observe all objects with G magnitude down to 20.7 mag during its five-year mission. The main goal of this mission is to make the largest, most precise three-dimensional map of the Milky Way (ESA 2017). Compared to the *Hipparcos* mission, *Gaia* will enable a factor of about 50 to 100 better in positional accuracy (up to the level of a few μas) and a factor of about 10 000 more in star number (more than 1 billion) (Gaia Collaboration et al. 2016b, Lindegren et al. 2018).

Quasars (quasi-stellar objects or QSOs) are extremely distant and small in apparent size. They are ideal objects for establishing a reference frame since they present no significant parallaxes or proper motions. The International Celestial Reference Frame (ICRF), which is the realization of the International Celestial Reference System (ICRS) at radio wavelengths (Arias et al. 1995), consists of 3414 such compact radio objects in its second realization (Fey et al. 2015a). *Gaia* will observe about 500 000 QSOs (Andrei et al. 2008), which will allow us to build a rotation-free celestial reference frame in the optical wavelengths and meet the ICRS criterion. Besides, the principle that *Gaia* uses two fields of view to observe might cause a global parallax bias in the *Gaia* catalog (van Leeuwen 2005; Butkevich et al. 2008; Butkevich et al. 2017, Liao et al. 2018). Since QSO parallaxes can be treated as zero, they are ideal objects to detect such bias.

Over the past few decades, surveys such as the 2dF Quasar Redshift Survey (2QZ) survey (Croom et al. 2004) and the Sloan Digital Sky Survey (SDSS) (Fukugita et al. 1996) contributed the majority of QSOs identified in optical wavelengths. Thousands of compact extragalactic sources have also been observed by the radio VLBI technique and they are listed in the ICRF2 (Boboltz et al. 2010), VLBA (Beasley et al. 2002; Fomalont et al. 2003), VLA (VLA 2009) and JVAS catalogs (Patnaik et al. 1992; Browne et al. 1998;Wilkinson et al. 1998). There are also QSOs that were discovered in X-ray wavelengths, such as the *Swift* X-ray Point Source catalog (Evans et al. 2014). Three decades ago, Veron-Cetty and Veron (Veron-Cetty & Veron 1989; Véron-Cetty & Véron 2006, 2010) gathered all those quasars into a single catalog (hereafter V&V), which has been updated since then until 2010. The latest version of their catalog included 133 336 quasars and 34 231 active galaxies. Souchay et al. (2009) compiled three successive versions of a quasar catalog designated as the Large Quasar Astrometric Catalog (LQAC) with the aim of providing useful astrometric data to all known quasars (Souchay et al. 2009, 2012, 2015). The latest version, LQAC3, which contains 321 957 objects, was published in early 2015. With the new data release of SDSS[1] (Abolfathi et al. 2018, Pâris et al. 2018), and surveys such as the Large Sky Area Multi-Object Fiber Spectroscopic Telescope (LAMOST) (Zhao 2012; Cui et al. 2012) and the *Wide-field Infrared Survey Explorer* (*WISE*) (Wright et al. 2010; Secrest et al. 2015), the number of quasars discovered in recent years has increased rapidly. The Million Quasars (MILLIQUAS) Catalog (Flesch 2017; Flesch 2015) compiles all the known or candidate active galactic nuclei (AGNs)/QSOs up to August 2017, which contains 1 998 464 objects including all-sky radio/X-ray associated objects.

Andrei et al. (2014) compiled the LQAC2 list, QSOs from SDSS Data Release 10 (DR10) and the Baryon Oscillation Spectroscopic Survey (BOSS) selection, as well as VLBI QSOs into the *Gaia* Initial QSO Catalog (GIQC). However, several reasons led us to implement a new compilation of the QSO catalog for the *Gaia* mission. First, the spatial uniformity of GIQC needs to be improved, see Figure 1 for the sky distribution of LQAC3. Second, to build up the *Gaia* reference frame and to detect any parallax bias in the *Gaia* catalog, it is crucial to maximize the number of QSOs in optical wavelengths. However, none of the current QSO catalogs are updated to the present date to include all the newly discovered QSOs: V&V contains the new QSOs discovered until 2010; LQAC has no QSOs from SDSS DR14, *WISE* or LAMOST DR5[2]; while MILLIQUAS missed the QSOs from LAMOST DR5. Third, false identification of QSOs may lead to an incorrect detection of the parallax bias. Catalogs such as MILLIQUAS include a large number of unconfirmed QSOs, which are not advisable for use in detecting parallax bias associated with the *Gaia* mission.

This paper is organized as follows: Section 2 introduces the data used, Section 3 is the compilation of QSOs and the last section is the discussion.

[1] See *http://www.sdss.org/dr14/* for more details.

[2] See *http://dr5.lamost.org* for more details.

2 DATA USED

The purpose of this compilation is to provide positions of known QSOs, which can be used to cross-match with *Gaia* observations. To maximize the number of QSOs/AGNs, we choose four samples from their huge number of reliable QSOs/AGNs. We start from the LQAC3 QSO list. LQAC3 contains all the known QSOs discovered in the 2dF/2QZ survey, the DR10Q of SDSS-III (Bolton et al. 2012; Pâris et al. 2014) and the VLBI QSOs listed in the ICRF2, VLBA, VLA and JVAS catalogs. Recently, LQAC4 was published by adding new quasars coming from the SDSS DR12Q into LQAC3 (Souchay et al. 2018, Gattano et al. 2018). Here in this compilation, the QSOs from SDSS in LQAC3 will be updated with the latest spectroscopically confirmed QSOs in the SDSS-DR14 Quasar Catalog (DR14Q) (Pâris et al. 2018) by using data from BOSS (Eisenstein et al. 2011; Dawson et al. 2013) and photometrically selected QSOs in SDSS. Then we add the spectroscopically confirmed QSOs in LAMOST DR5 using LAMOST spectroscopic data. Finally, we complement the mid-infrared (IR) color selected AGNs from the *WISE* data (Wright et al. 2010; Secrest et al. 2015).

2.1 The Large Quasar Astrometric Catalog

The LQAC3 catalog is the latest version of the three successive compilations of known quasars in catalogs, which contains 321 957 objects including 14 128 AGNs and 1183 BL Lacs. It was built by carrying out the cross-identification between existing catalogs of quasars chosen for their huge number of objects up to 2015. LQAC3 includes all the available data related to magnitudes, radio fluxes and redshifts. The sky density distribution of LQAC3 is shown in Figure 1 and the composition can be found in Table 1.

2.2 The SDSS QSO Catalog

The SDSS is a large imaging and spectroscopic survey, which uses the Sloan Foundation's 2.5 m optical telescope at Apache Point Observatory in New Mexico for the northern sky survey and the 2.5 m du Pont optical telescope at Las Campanas Observatory in Chile after being extended to the southern sky. It has progressed through four

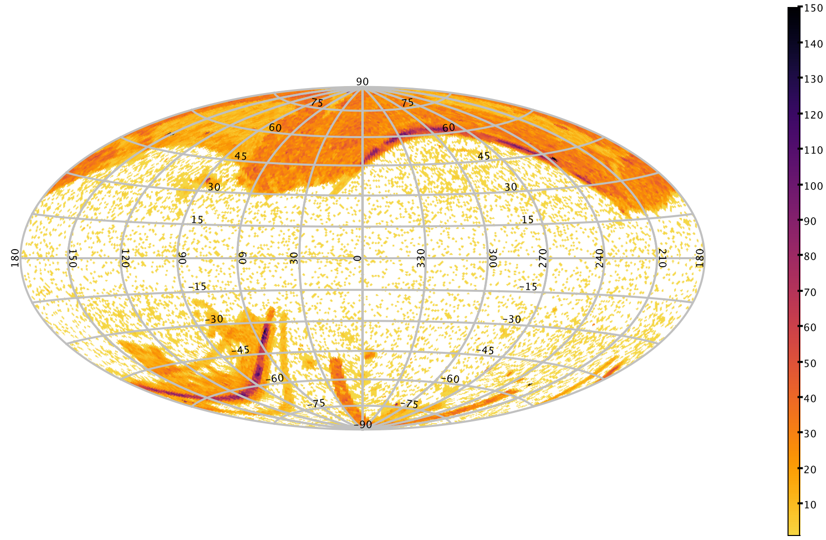

Fig. 1 The density distribution plot of the LQAC3 sample of AGN/QSO sources. The map shows the sky density with each cell representing approximately 0.84 deg^2, using the Hammer-Aitoff projection in Galactic coordinates with zero longitude at the center and increasing longitude from right to left.

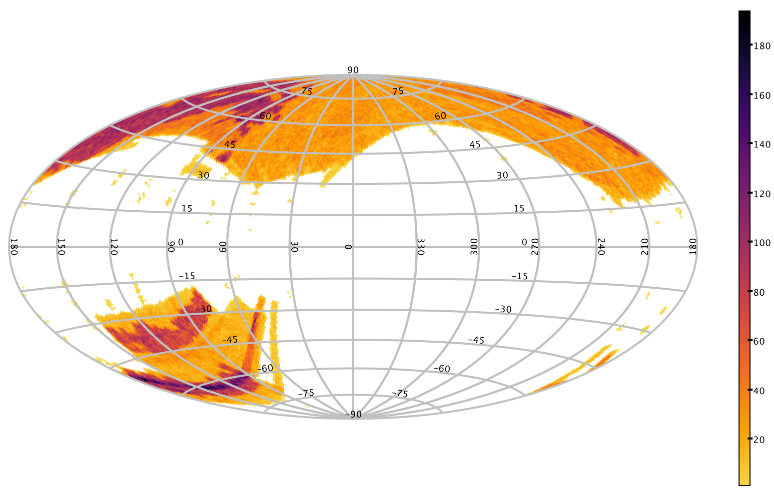

Fig. 2 The density distribution plot of the SDSS DR14Q sample of QSO sources. The map shows the sky density of each cell representing approximately 0.84 deg^2, using the Hammer-Aitoff projection in Galactic coordinates with zero longitude at the center and increasing longitude from right to left.

phases including SDSS-I (2000–2005), SDSS-II (2005–2008), SDSS-III (2008–2014) and SDSS-IV (2014–2020). DR14Q used here comes from the second data release of the extended Baryon Oscillation Spectroscopic Survey (eBOSS) (Eisenstein et al. 2011; Dawson et al. 2013) from SDSS-IV. This catalog includes all SDSS-IV/eBOSS objects that were spectroscopically targeted as quasar candidates and that were confirmed as quasars (Pâris et al. 2018). The SDSS DR14Q quasar catalog also contains all the quasars observed as part of SDSS-I/II/III. The total number of QSOs in SDSS DR14Q is 526 356. For each object, the catalog presents five-band (u, g, r, i, z) CCD-based photometry. Most of the QSOs are distributed near the North Galactic Cap and South Galactic Cap. See Figure 2 for the spatial density distribution.

2.3 The QSOs in LAMOST DR5

LAMOST is a reflecting Schmidt telescope with a wide field of view of 5° in diameter and an effective aperture of about 4 m (Zhao 2012; Cui et al. 2012), which can record 4000 celestial object spectra simultaneously with its 4000 fibers. The telescope began its first spectroscopic regular survey in September 2012. The fifth data release (DR5) was published online in late 2017, which included 51 133 quasars in the LAMOST general catalog. Due to

Table 1 Number of Quasars from Each Catalog in LQAC3 Compilation

Origin	Flag	Nature	Number
ICRF2	A	radio	3414
VLBA	B	radio	7213
VLA	C	radio	1858
JVAS	D	radio	2118
SDSS	E	optical	262 535
2QZ	F	optical	23 660
2df-SDSS LRG	G	optical	9058
FIRST	H	radio	969
HB	I	optical and radio	6720
V&V	M	optical and radio	79 692

Notes: This table is taken from the LQAC3 paper (Souchay et al. 2015). The HB catalog is the abbreviation of the Hewitt & Burbidge catalog (Hewitt & Burbidge 1993).

the lack of a systematic spectroscopic survey, the number of spectroscopically confirmed quasars remains very small in low Galactic latitudes. With the help of the LAMOST Spectroscopic Survey of the Galactic Anti-center (LSS-GAC) (Liu et al. 2014; Yuan et al. 2015), 151 unique quasars identified from LAMOST toward the anti-center of the Galaxy were discovered (Huo et al. 2017). These quasars from LAMOST will play an important role in the proper motion and parallax validation of *Gaia* results in the highly dust extinct Galactic disk regions. See Figure 3 for the sky density distribution.

2.4 The *WISE* AGN Catalog

WISE (Wright et al. 2010) is a satellite with a 40 cm aperture that was launched by NASA in December 2009, and begun its survey in January 2010 and finished the first all-sky cryogenic survey in August 2010. After that, an additional 30% of the sky was mapped from September 2010 to February 2011. The satellite scanned the whole sky in mid-IR at 3.4, 4.6, 12 and 22 μm (W1, W2, W3, and W4, respectively). Sources in the *WISE* catalog are classified as AGNs from a two-color IR photometric criterion with observations representing *WISE* data (Secrest et al. 2015). This catalog (mid-IR AGNs, abbreviated as MIRAGNs) contains the all-sky sample of 1.4 million sources. As estimated by the author, the probability of a star that is detected in this optical survey being misidentified as a QSO is smaller than 0.041% per source, which makes MIRAGNs highly promising for celestial reference frame work due to its huge number of uniformly spatially distributed compact extragalactic sources. The sky density distribution of MIRAGNs is shown in Figure 4.

3 THE COMPILATION

3.1 Cross-identifications between Catalogs

The criterion for being identified as the same object in the cross-identifications is the angular distance between two objects being smaller than a certain value. As shown in Figure 5, the majority of the angular distances between two objects is smaller than $2''$. The larger the angular distance is, the higher the possibility of false identifications becomes. Thus, the search radius of angular distance in cross-identifications is set to $2''$. Even so, the risk of finding a false pair or missing identification is unavoidable. In this situation, the redshift information can be used as the second criterion, as adopted in the construction of LQAC (Souchay et al. 2009). A significant difference in redshift values indicates that the sources in this pair are two different ones, while close values suggest that they are only one source with slightly different positions in the original catalogs.

3.2 The Final Catalog

The final catalog (designated as Known Quasars Catalog for *Gaia* mission, KQCG) contains 1 842 076 QSOs. The spatial distribution of these objects is shown in Figure 6. The higher density area in the figure is because of the deeper coverage of the SDSS and LAMOST survey areas near the North/South Galactic Cap. The average density of the sky distribution is about 45 objects per degree^2. The SDSS DRQ14 and MIRAGNs catalogs contribute the majority of optical QSOs in this compilation. See Table 2 for the composition of the final catalog. The redshifts of the final catalog are shown in the right panel of Figure 7. One can see that the redshifts of these QSOs are below $z = 4$. The histogram of the magnitude in the R band (the effective wavelength midpoint of the R band is $\lambda_{\rm eff} \approx 658\,{\rm nm}$) is shown in the left panel of Figure 7. About 15% of the sources are fainter than R magnitude 21, which may be beyond the observation limit of *Gaia* (complete to G magnitude 20.7).

Figures 8 and 9 display the sky coverage of the final catalog with respect to the equatorial and Galactic coordinates, respectively. In the left panel of Figure 8, the two depleted zones $[70° - 120°]$ and $[260° - 310°]$ are due to crossing the Galactic plane. The detection is more abundant in the northern hemisphere than in the southern part in equatorial coordinates, which is clearly visible in the right panel of Figure 8. The distribution of sources is rather homogenous with respect to Galactic longitude. Due to the

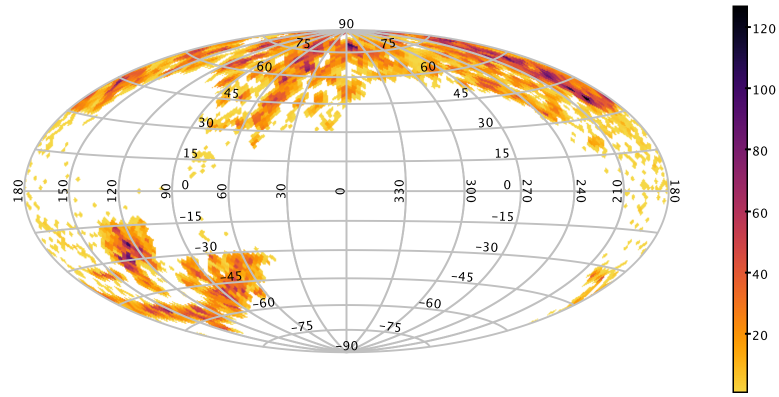

Fig. 3 The density distribution plot of AGN/QSO sources in LAMOST DR5. The map shows the sky density with each cell representing approximately $0.84\,\mathrm{deg}^2$, using the Hammer-Aitoff projection in Galactic coordinates with zero longitude at the center and increasing longitude from right to left.

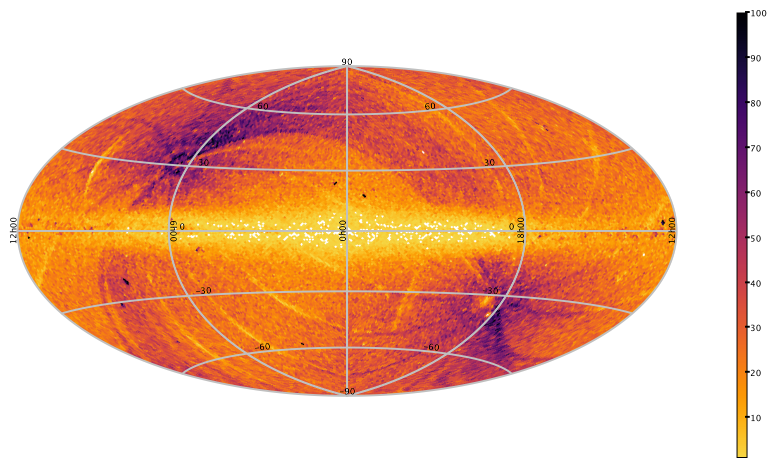

Fig. 4 Density plot of the *WISE* sample of AGN/QSO sources. The map shows the sky density with each cell representing approximately $0.84\,\mathrm{deg}^2$, using the Hammer-Aitoff projection in Galactic coordinates with zero longitude at the center and increasing longitude from right to left. As indicated by the author, the over-density of sources at the ecliptic poles is due to deeper *WISE* coverage, while the under-abundance along the Galactic plane is due to source confusion (Secrest et al. 2015).

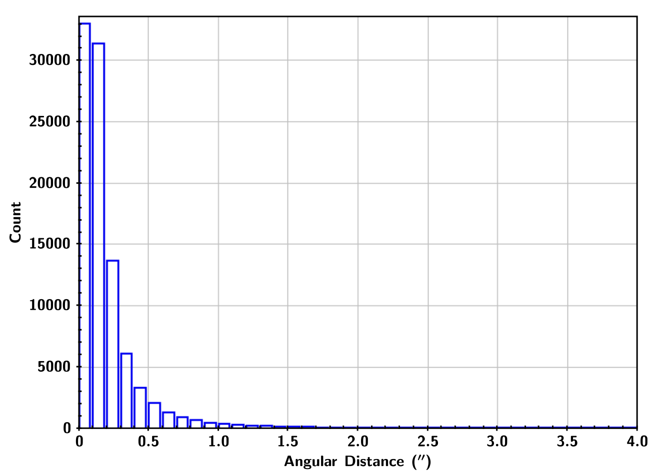

Fig. 5 Histogram of angular distance of the cross-identified quasars between the LQAC3 and MIRAGNs samples. The abscissa is the angular distance between two identified targets and the ordinate is the number of matches.

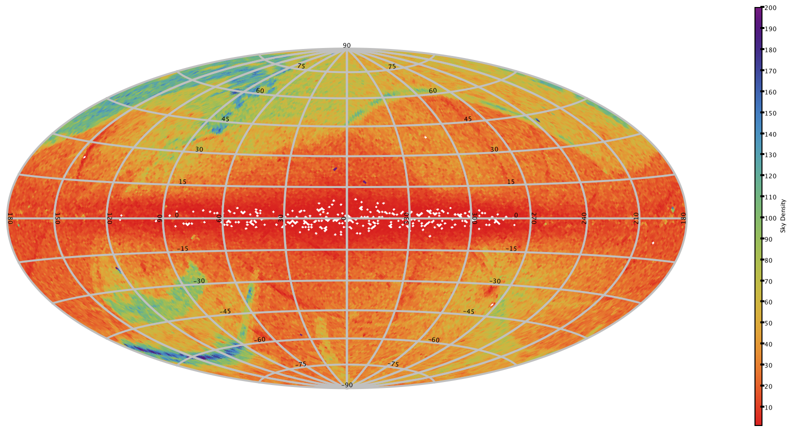

Fig. 6 The sky density distribution of the final QSO catalog. The map shows the sky density with each cell representing approximately $0.84\,\text{deg}^2$, using the Hammer-Aitoff projection in Galactic coordinates with zero longitude at the center and increasing longitude from right to left.

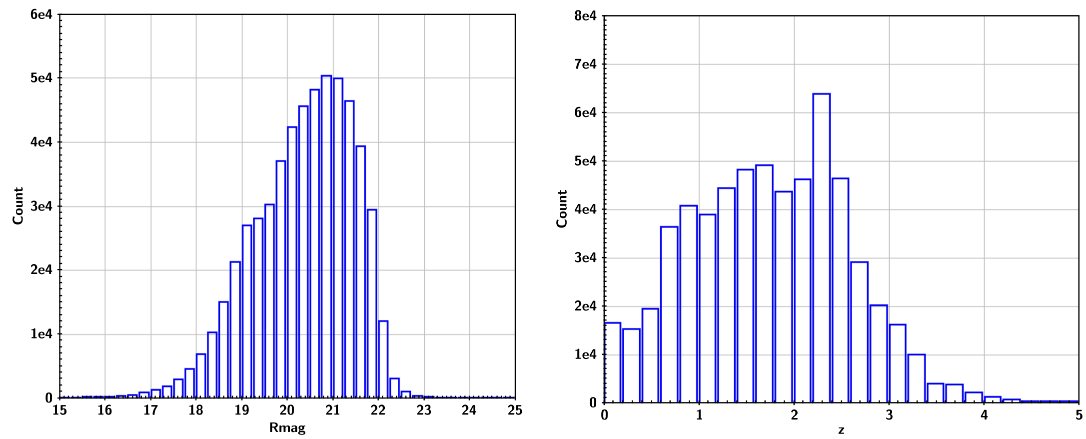

Fig. 7 Histogram of magnitude in the R band (*left*) and redshift distribution of the final compiled (*right*) sample of AGN/QSO sources.

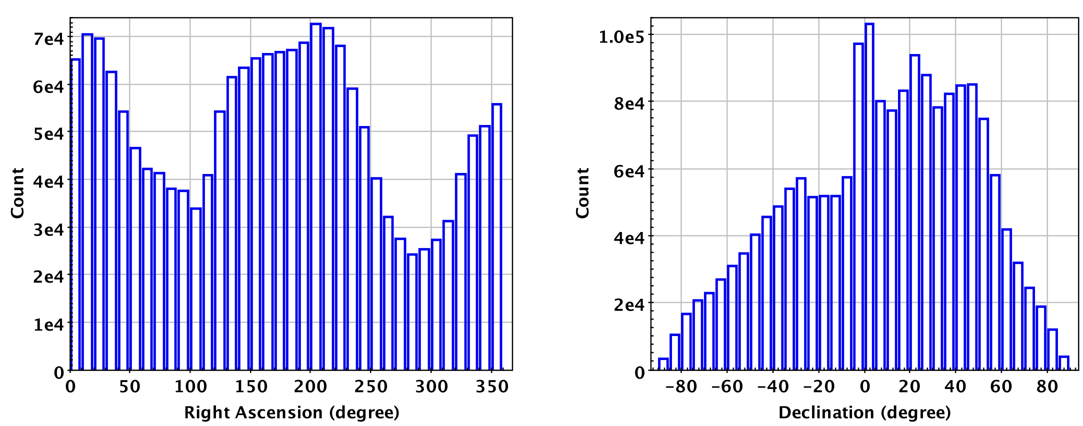

Fig. 8 Histogram of the number of AGN/QSO sources in KQCG with respect to right ascension (*left*) and declination (*right*).

relatively small area near the poles and lack of sources near the Galactic plane, the distribution of sources drops drastically in the neighborhood of the Galactic plane and the Galactic pole, as shown in Figure 9.

3.3 Description of the Final Catalog

The final catalog contains 1 842 076 objects in total. A large number of them come from the *WISE* and SDSS surveys. An example of this final catalog is shown in Table 3.

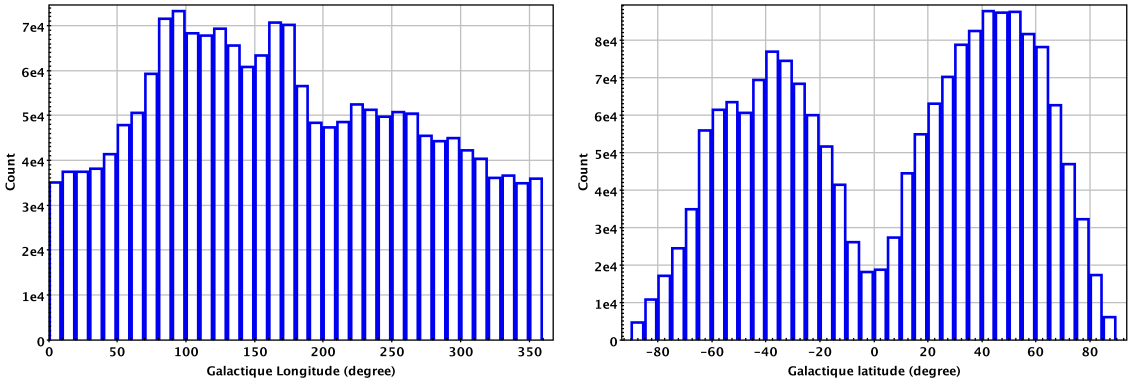

Fig. 9 Histogram of the number of AGN/QSO sources in KQCG with respect to Galactic longitude (*left*) and Galactic latitude (*right*).

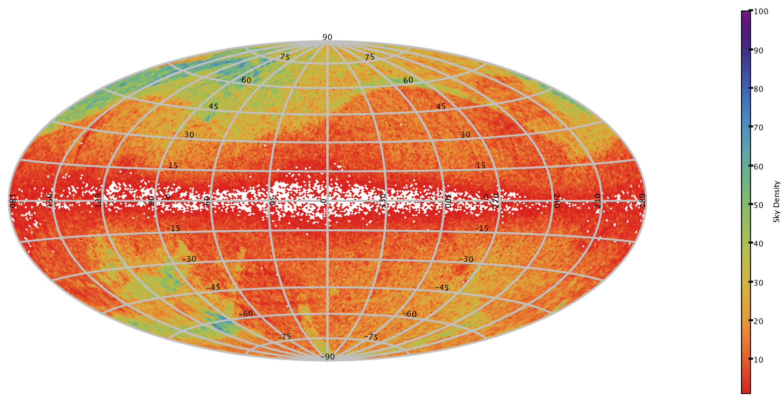

Fig. 10 Sky density distribution of the QSOs in KQCG found in *Gaia* DR1. The map shows the sky density with each cell representing approximately 0.84 deg^2, using the Hammer-Aitoff projection in Galactic coordinates with zero longitude at the center and increasing longitude from right to left.

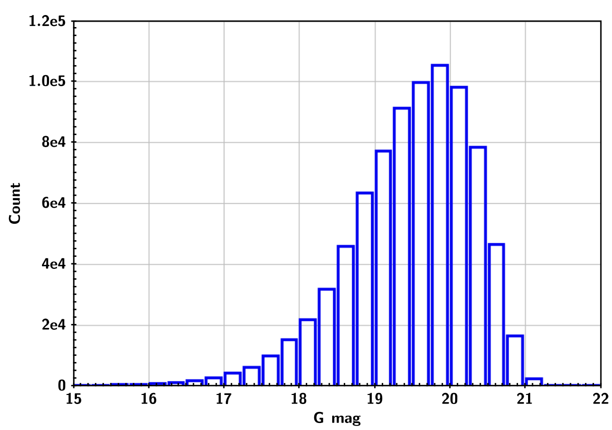

Fig. 11 Histogram of *Gaia* G magnitude of AGN/QSO sources after cross-matching the KQCG with *Gaia* DR1.

The complete KQCG catalog is also available in electronic form at the CDS via anonymous ftp to *cdsarc.u-strasbg.fr* or via *http://cdsweb.u- strasbg.fr*.

4 DISCUSSION

We compiled known QSOs from the LQAC3, SDSS DR14Q and LAMOST DR5 QSO catalogs, and MIRAGNs from the *WISE* survey. The final catalog contains 1 842 076 objects, among which there are 1 762 067 objects with position uncertainty information from their original catalogs. To evaluate the possible detected QSOs from this catalog in the *Gaia* mission, we cross match this catalog with the *Gaia* DR1 catalog (Gaia Collaboration et al. 2016a; Lindegren et al. 2016). The cross-match criterion is set to

Table 2 Number of Quasars from Each Catalog after Compilation in KQCG

Origin	Ref/Flag	Nature	Number	Number found in *Gaia* DR1
ICRF2	A	radio	3414	2372
VLBA	B	radio	7213	4450
VLA	C	radio	1858	1269
JVAS	D	radio	2118	1406
SDSS	E	optical	499127	245982
2QZ	F	optical	23660	18203
2df-SDSS LRG	G	optical	9058	2476
FIRST	H	radio	969	920
HB	I	optical and radio	6720	6064
V&V	M	optical and radio	79692	7584
LAMOST	O	optical	24666	22252
MIRAGNs	P	optical	1260635	519412

Notes: The reference/flag symbols are adopted from LQAC3, with ‘O’ (LAMOST) and ‘P’ (MIRAGNs) being the two new symbols. The objects found in *Gaia* DR1 will be added with a flag “Q”.

Table 3 A Sample Showing a Few Lines of the Final Catalog KQCG

Name (1)	RA_Deg (2)	Dec_Deg (3)	eRA (4)	eDEC (5)	z (6)	U mag (7)	G mag (8)	R mag (9)	I mag (10)	Z mag (11)	Ref (12)	W1-W2 (13)	W2-W3 (14)	W1_Mag (15)
081007.25+551542.3	122.5302084	55.26177771	0.026286836	0.029817969	2.6643622	21.0	21.0	21.0	21.0	21.0	E			
003648.66-032744.4	9.202785691	–3.462339742	0.0158835453	0.0145377308	1.8971459	21.0	21.0	21.0	20.0	20.0	E			
082613.65+381053.5	126.5568801	38.18153128	0.016854173	0.0169042417	0.7296067	22.0	23.0	21.0	22.0	21.0	E			
084316.61+365209.6	130.8192082	36.86933754	0.0079763228	0.00782948	1.0963088	21.0	20.0	20.0	20.0	20.0	E			
235509.79+334154.2	358.7908056	33.69839878	0.0077585033	0.008040454	2.928	22.0	21.0	20.0	20.0	20.0	E			
215016.00+260431.0	327.5666858	26.07528648	0.026640975	0.0246672213	1.4373662	21.0	20.0	20.0	20.0	20.0	E			
023511.82+044525.2	38.79926061	4.757013574	0.067718781	0.060872302	1.7565038	22.0	22.0	21.0	21.0	21.0	E			
002218.04+205639.5	5.575188182	20.94432624	0.0252669286	0.0227453122	1.9788945	21.0	21.0	20.0	20.0	20.0	E			
023943.45+002951.6	39.93108184	0.497667553	0.0335679416	0.0323431963	1.877	22.0	22.0	22.0	22.0	21.0	E			
225723.83+164123.6	344.3492949	16.68991206	0.00393273449	0.0036682014	2.571	19.0	19.0	19.0	19.0	18.0	E			

Notes: Only a portion of the table is shown here for illustration. The whole table containing information on all quasars is available in the online electronic version at *http://www.raa-journal.org/docs/Supp/KQCG.csv.*

- Column (1) gives the reference name of the quasar in the catalog. If there is a name from its original catalog, the original name is used. Otherwise, it will be designated by its equatorial coordinates calculated in degrees and truncated to the arcsecond level.
- Columns (2) and (3) are the equatorial coordinates (α, δ) of the object given by the original catalog.
- Columns (4) and (5) are the position uncertainties $(\sigma_\alpha, \sigma_\delta)$ of the object (in arcsec). These uncertainties come from their original catalogs. When the the position uncertainty is not available, the value will be left empty.
- Column (6) gives the redshift value z of each quasar.
- Columns (7) to (11) give the apparent magnitudes in the u, g, r, i and z bands, respectively. These photometric values come from their original catalogs. When the magnitude is not available, the value will be left empty.
- Column (12) provides the reference catalog or flag indicating the presence of the quasar in one of the 12 catalogs from A to P as LQAC3 does, see Table 2.
- Columns (13)–(15) give the W1, W2 and W3 magnitude information on the sources from MIRAGNs.

$2''$, and 797 632 objects are found. Among these objects, 5368 objects are identified as radio QSOs in LQAC3. The sky density distribution can be found in Figure 10 and the histogram of their *Gaia* G magnitudes can be found in Figure 11.

This compilation of QSOs can be used in conjunction with the *Gaia* mission in the following three ways: (1) They can be selected to build the *Gaia* celestial reference frame. With such a large number of QSOs and uniform spatial distribution, after cross-matching with *Gaia* data, one can statistically analyze the overall properties of this new celestial reference frame with respect to their spatial distribution, accuracy and magnitude distribution. (2) As the parallaxes and proper motions of the QSOs can be treated as zero, they can be used to detect the parallax bias in the *Gaia* catalog and as additional quality indicators to evaluate the overall quality of the *Gaia* catalog. (3) A comparison of QSOs in radio wavelengths with their optical counterparts can be made between the *Gaia* solution and the VLBI solution. More importantly, comparing QSOs in radio wavelengths with their optical counterparts can be used as a link between ICRF in the radio and optical bands.

Acknowledgements This work has made use of data from the European Space Agency (ESA) mission *Gaia*, processed by the *Gaia* Data Processing and Analysis Consortium (DPAC). The author is grateful to the developers of TOPCAT (Taylor 2005) for their software. This publication makes use of data products from the *Wide-field Infrared Survey Explorer*, which is a joint project of the University of California, Los Angeles, and the Jet Propulsion Laboratory/California Institute of Technology, funded by the National Aeronautics and Space Administration. The Guo Shou Jing Telescope (the Large Sky Area Multi-Object Fiber Spectroscopic Telescope, LAMOST) is a National Major Scientific Project built by the Chinese Academy of Sciences. Funding for the project has been provided by the National Development and Reform Commission. LAMOST is operated and managed by the National Astronomical Observatories, Chinese Academy of Sciences. This work has been supported by grants from the National Natural Science Foundation of China (Grant Nos. 11703065 and 11573054).

References

Abolfathi, B., Aguado, D. S., Aguilar, G., et al. 2018, ApJS, 235, 42
Andrei, A. H., Assafin, M., Barache, C., et al. 2008, in IAU Symposium, 248, A Giant Step: from Milli- to Micro-arcsecond Astrometry, eds. W. J. Jin, I. Platais, & M. A. C. Perryman, 260
Andrei, H., Antón, S., Taris, F., et al. 2014, in Journées 2013 “Systèmes de référence spatio-temporels”, ed. N. Capitaine, 84
Arias, E. F., Charlot, P., Feissel, M., & Lestrade, J.-F. 1995, A&A, 303, 604
Beasley, A. J., Gordon, D., Peck, A. B., et al. 2002, ApJS, 141, 13
Boboltz, D. A., Gaume, R. A., Fey, A. L., et al. 2010, in Bulletin of the American Astronomical Society, 42, American Astronomical Society Meeting Abstracts #215, 512
Bolton, A. S., Schlegel, D. J., Aubourg, É., et al. 2012, AJ, 144, 144
Browne, I. W. A., Wilkinson, P. N., Patnaik, A. R., & Wrobel, J. M. 1998, MNRAS, 293, 257
Butkevich, A. G., Klioner, S. A., Lindegren, L., Hobbs, D., & van Leeuwen, F. 2017, A&A, 603, A45
Butkevich, A. G., Klioner, S. A., Lindegren, L., & van Leeuwen, F. 2008, GAIA-CA-TN-LO-AGB-006-1, *http://www.cosmos.esa.int/web/gaia/ public-dpac-documents*
Croom, S. M., Smith, R. J., Boyle, B. J., et al. 2004, MNRAS, 349, 1397
Cui, X.-Q., Zhao, Y.-H., Chu, Y.-Q., et al. 2012, RAA (Research in Astronomy and Astrophysics), 12, 1197
Dawson, K. S., Schlegel, D. J., Ahn, C. P., et al. 2013, AJ, 145, 10
Eisenstein, D. J., Weinberg, D. H., Agol, E., et al. 2011, Astronomical Journal, 142, 725
ESA. 2017, Gaia Mission Summary, *http://sci.esa.int/jump.cfm?oid=28820*, accessed April 21, 2017
Evans, P. A., Osborne, J. P., Beardmore, A. P., et al. 2014, ApJS, 210, 8
Fey, A. L., Gordon, D., Jacobs, C. S., et al. 2015a, AJ, 150, 58
Flesch, E. W. 2015, PASA, 32, e010
Flesch, E. W. 2017, VizieR Online Data Catalog, 7277
Fomalont, E. B., Petrov, L., MacMillan, D. S., Gordon, D., & Ma, C. 2003, AJ, 126, 2562
Fukugita, M., Ichikawa, T., Gunn, J. E., et al. 1996, AJ, 111, 1748
Gaia Collaboration, Brown, A. G. A., Vallenari, A., et al. 2016a, A&A, 595, A2
Gaia Collaboration, Prusti, T., de Bruijne, J. H. J., et al. 2016b, A&A, 595, A1
Gattano, C., Andrei, A. H., Coelho, B., et al. 2018, A&A, 614, A140
Hewitt, A., & Burbidge, G. 1993, ApJS, 87, 451
Huo, Z.-Y., Liu, X.-W., Shi, J.-R., et al. 2017, RAA (Research in Astronomy and Astrophysics), 17, 032
Liao, S., Lattanzi, M. G., Vecchiato, A., et al. 2018, in IAU Symposium, 330, Astrometry and Astrophysics in the Gaia Sky, ed. A. Recio-Blanco, P. de Laverny, A. G. A. Brown, & T. Prusti, 231
Lindegren, L., Lammers, U., Bastian, U., et al. 2016, A&A, 595, A4
Lindegren, L., Hernández, J., Bombrun, A., et al. 2018, A&A, 616, A2
Liu, X.-W., Yuan, H.-B., Huo, Z.-Y., et al. 2014, in IAU Symposium, 298, Setting the Scene for Gaia and LAMOST, eds. S. Feltzing, G. Zhao, N. A. Walton, & P. Whitelock, 310
Pâris, I., Petitjean, P., Aubourg, É., et al. 2014, A&A, 563, A54
Pâris, I., Petitjean, P., Aubourg, É., et al. 2018, A&A, 613, A51
Patnaik, A. R., Browne, I. W. A., Wilkinson, P. N., & Wrobel, J. M. 1992, MNRAS, 254, 655
Perryman, M. A. C., Lindegren, L., Kovalevsky, J., et al. 1997, A&A, 323, L49

Secrest, N. J., Dudik, R. P., Dorland, B. N., et al. 2015, ApJS, 221, 12

Souchay, J., Andrei, A. H., Barache, C., et al. 2012, A&A, 537, A99

Souchay, J., Andrei, A. H., Barache, C., et al. 2018, in IAU Symposium, 330, Astrometry and Astrophysics in the Gaia Sky, eds. A. Recio-Blanco, P. de Laverny, A. G. A. Brown, & T. Prusti, 75

Souchay, J., Andrei, A. H., Barache, C., et al. 2009, A&A, 494, 799

Souchay, J., Andrei, A. H., Barache, C., et al. 2015, A&A, 583, A75

Taylor, M. B. 2005, in Astronomical Society of the Pacific Conference Series, 347, Astronomical Data Analysis Software and Systems XIV, ed. P. Shopbell, M. Britton, & R. Ebert, 29

van Leeuwen, F. 2005, A&A, 439, 805

Veron-Cetty, M.-P., & Veron, P. 1989, European Southern Observatory Scientific Report, 7, 1

Véron-Cetty, M.-P., & Véron, P. 2006, A&A, 455, 773

Véron-Cetty, M.-P., & Véron, P. 2010, A&A, 518, A10

VLA. 2009, VLA Calibrator Manual, *http://www.vla.nrao.edu/astro/calib/manual/*, modified on Saturday, 21-May-2016

Wilkinson, P. N., Browne, I. W. A., Patnaik, A. R., Wrobel, J. M., & Sorathia, B. 1998, MNRAS, 300, 790

Wright, E. L., Eisenhardt, P. R. M., Mainzer, A. K., et al. 2010, AJ, 140, 1868

Yuan, H.-B., Liu, X.-W., Huo, Z.-Y., et al. 2015, MNRAS, 448, 855

Zhao, G., Zhao, Y. H., Chu, Y. Q., et al., 2012, RAA (Research in Astronomy and Astrophysics), 12, 723